Resistance of the boreal forest to high burn rates

Jessie Héon[a], Dominique Arseneault[a,1], and Marc-André Parisien[b]

[a]Département de biologie, chimie et géographie, Centre d'études nordiques, Université du Québec à Rimouski, Rimouski, QC, Canada G5L 3A1; and [b]Northern Forestry Centre, Canadian Forest Service, Natural Resources Canada, Edmonton, AB, Canada T6H 3S5

Edited by William J. Bond, University of Cape Town, South Africa, and approved August 4, 2014 (received for review May 23, 2014)

Boreal ecosystems and their large carbon stocks are strongly shaped by extensive wildfires. Coupling climate projections with records of area burned during the last 3 decades across the North American boreal zone suggests that area burned will increase by 30–500% by the end of the 21st century, with a cascading effect on ecosystem dynamics and on the boreal carbon balance. Fire size and the frequency of large-fire years are both expected to increase. However, how fire size and time since previous fire will influence future burn rates is poorly understood, mostly because of incomplete records of past fire overlaps. Here, we reconstruct the length of overlapping fires along a 190-km-long transect during the last 200 y in one of the most fire-prone boreal regions of North America to document how fire size and time since previous fire will influence future fire recurrence. We provide direct field evidence that extreme burn rates can be sustained by a few occasional droughts triggering immense fires. However, we also show that the most fire-prone areas of the North American boreal forest are resistant to high burn rates because of overabundant young forest stands, thereby creating a fuel-mediated negative feedback on fire activity. These findings will help refine projections of fire effect on boreal ecosystems and their large carbon stocks.

climate change | fire-free intervals | fuel feedback | probability of burning | tree ring dating

Disturbances are likely to modulate the response of forest ecosystems to future climate change (1, 2). This is particularly true in the North American boreal forest, which is shaped by large and severe wildfires. Because most fires are stand-replacing, burn rates (percentage area burned annually) determine forest age, as well as structure and composition at site and landscape levels, and drive the regional carbon balance (3–5). Models suggest this biome will experience rapid temperature increases during the 21st century, with a potential 30–500% increase in burn rates (6–9). Both fire size and the frequency of large fire years are expected to increase (8, 10, 11), with a cascading effect on ecosystem dynamics (12–16) and carbon storage (17–21).

Indeed, several boreal forest ecosystems are not resilient to fire disturbance when burn rates are high. Large and severe fires may alter seed sources and seedbeds for tree recruitment, which may trigger shifts to novel forest ecosystems (14, 22). In addition, shortened fire-free intervals (FI) may shift young, sexually immature tree populations to faster-maturing species (12, 23–25). Large and severe fires and short FIs also erode the accumulated carbon stocks (19, 21). Because boreal fires can become immense (>100 km long) (26, 27), fire-mediated climate change can trigger extensive and abrupt ecosystems responses.

Together, fire size and FI determine how fires recur and overlap across boreal landscapes. If fires spread and overlap independent of time since previous fire (TSF), then burn rates are not limited by fuel availability and forest survivorship decreases exponentially with TSF (3). In this situation, the boreal forest would be vulnerable (i.e., exposed and sensitive) to future increases in burn rates because the surface area experiencing short FIs would increase disproportionately relative to that of longer intervals. Conversely, if the probability of burning increases with fuel recovery, resistance would develop against large fires and against short FIs, thus attenuating the vulnerability of the boreal forest to high burn rates.

The role of fuel age on burn rates has long been debated with regard to the North American boreal forest. Sequences of overlapping fires are difficult to reconstruct, as earlier fires are often masked by later ones, especially where fires are large, severe, and frequent. As a consequence, the influence of earlier fires on the occurrence of subsequent ones is poorly documented. In the absence of data on fire overlaps, it has been widely assumed that the effect of fuel age is negligible or short-lasting (less than 20 y), mostly based on a few localized studies (28). However, a recent analysis of the detailed Canadian fire record of the last 31 y suggests that recent burns have negatively influenced subsequent fire activity across landscapes (29). Direct field evidences from the Scandinavian boreal forest (30, 31) and high-resolution charcoal records from Alaskan lakes also suggest that the risk of burning increases with TSF during the first 40–50 postfire years (32, 33).

In this study, we first developed a new approach to reconstructing the length of overlapping fires along a 190-km-long transect, thus allowing the systematic reconstruction of fire size and FIs during the last 200 y in one of the most fire-prone regions of the North American boreal forest. We used this data set to examine how fire size and FIs vary in space and time and to verify, from direct field evidence, whether or not the probability of burning increases with TSF. This allowed us to assess the degree at which the boreal forest is resistant to large fires and short FIs. We subsequently used the recorded fire polygons of the last 31 y (1980–2010) to examine whether the results obtained from our main study region could be extended to the rest of the North American boreal forest.

Significance

Climate change is expected to drastically increase both fire size and the frequency of large-fire years in the North American boreal forest, with consequent effects on forest ecosystems and carbon stocks. However, the influence of fire size and time since previous fire on fire activity is poorly understood because of incomplete records of past fire overlaps. Here we reconstruct the length of overlapping fires during the last 200 years along a 190-km transect and provide direct field evidence that extreme burn rates can be sustained by occasional droughts triggering immense fires. Fire occurrence in the most fire-prone regions of the North American boreal forest is, however, already fuel-limited and will resist further climate change because of overabundant young forest stands.

Author contributions: J.H. and D.A. designed research; J.H., D.A., and M.-A.P. performed research; J.H., D.A., and M.-A.P. analyzed data; and D.A. wrote the paper.

The authors declare no conflict of interest.

This article is a PNAS Direct Submission.

Data deposition: The data reported in this paper have been deposited to the National Oceanic and Atmospheric Administration (NOAA) paleofire database, http://ncdc.noaa.gov (accession no. 17054).

[1]To whom correspondence should be addressed. Email: dominique_arseneault@uqar.ca.

This article contains supporting information online at www.pnas.org/lookup/suppl/doi:10.1073/pnas.1409316111/-/DCSupplemental.

Results and Discussion

Using tree ring dating of tree establishment dates and fire-scarred trees (Fig. S1), we obtained $n = 1836$ fire dates in 93 contiguous ~2 × 1 km cells along a road transect in the unmanaged boreal forest of eastern Canada (Fig. S2), which revealed 64 distinct fire years between 1617 and 2013 (Fig. S3). Although the number of fire years per decade generally decreased after 1900 (almost a twofold decrease in 1900–2013 compared with the 1800–1899 period; Mann–Whitney U test; $P = 0.01$), the largest fires became much larger after 1920 (Figs. 1*D* and 2*A*). Burned lengths along the transect were very high during the decades of 1920, 1940, 1970, 1980, and 2010 because of the extremely large fires of 1922 (118 km), 1941 (91 km), 1972 (62 km), 1989 (96 km), and 2013 (59 km). The burn rate almost doubled, going from 1.4% of the land area y^{-1} between 1810 and 1909 to 2.4% y^{-1} between 1910 and 2013 (Fig. 2*B*).

The largest fires (length > 10 km) of the 20th century generally correspond to major peaks in the July mean Drought Code (DC) (35), indicating they mostly occurred during extreme droughts (Fig. 2*C*). Our study thus shows how occasional drought years may translate into a succession of immense fires, generating large expanses of young forest stands and thereby shifting the landscape age structure across boreal landscapes. Drought conditions during 1922, 1941, 1972, and 1989 have resulted in a total of 367 km of burns along our transect, corresponding to 81% of the total length burned during the last century. The overlapping areas of these fires have greatly increased the proportion of short FIs and young forest stands and have shifted the age class distribution to a strong dominance of cells younger than 50 y (Figs. 1*D*, 2*B*, and 3*A*). Considering that trees in our study area continue to grow in height for at least 70 y after a fire (Fig. 4), the shifting landscape age structure implies a regional decline of aboveground biomass and carbon storage over multiple disturbance–recovery episodes during the 20th century (36).

The observed drought-induced, fire-mediated biomass reduction caused a negative feedback on subsequent burn rates. In theory, if the probability of burning is age-independent, then the TSF and FI frequency distributions are similar across landscapes (i.e., the FI/TSF ratio is constant across age classes and equal to the overall burn rate), and both distributions decrease exponentially (37, 38). In contrast to these expectations, FI frequencies increased with interval length during the 1810–1909 and 1910–2013 periods (Fig. 3*B*), indicating that forest stands less than ~50 y old burned less frequently than expected during each period (Fig. 3*C*). In addition, the burn rate shifted from slightly to strongly dependent on TSF when it increased after 1910 (Fig. 3*C*). Relative to the period before 1910, the burn rate increased much more rapidly for stands 25–50 y old, indicating that during the 20th century, insufficient time for fuel recovery limited fire spread across cells younger than ~50 y. Indeed, the increasing probability of burning with TSF reflects the postfire trend of fuel accumulation in these landscapes (Figs. 3*C* and 4*B*) and is similar to trends deduced from field studies in Scandinavia (30, 31) and from high-resolution charcoal records in Alaskan lakes (32, 33). The large fires of 1916, 1922, and 1941 almost completely burned the study transect during the early 20th century, increasing the landscape resistance to subsequent fires (Fig. 1*D*). Despite drought peaks in 1947, 1955, 1961, 1963, 1966, and 1968 (Fig. 2*C*), the next large fire after 1941 occurred only in 1972, in an area that previously burned 50 y earlier in 1922. This burn-rate feedback during the 20th century is also evidenced by the decreasing number of fire years per decade and by the alternation of peaks and troughs in burn lengths. The decades of 1920, 1940, 1970, 1980, and 2010 had the longest burn lengths, whereas the intervening decades of 1930, 1960, 1990, and 2000 were all among the 6 decades with the shortest burn lengths since 1810 (Fig. 2*A*).

Overlaps between the fires of 1916 and 1922, as well as between the fires of 1922 and 1941 and the fires of 1972 and 1989, generated short FIs of 6–20 y in several cells, indicating that young

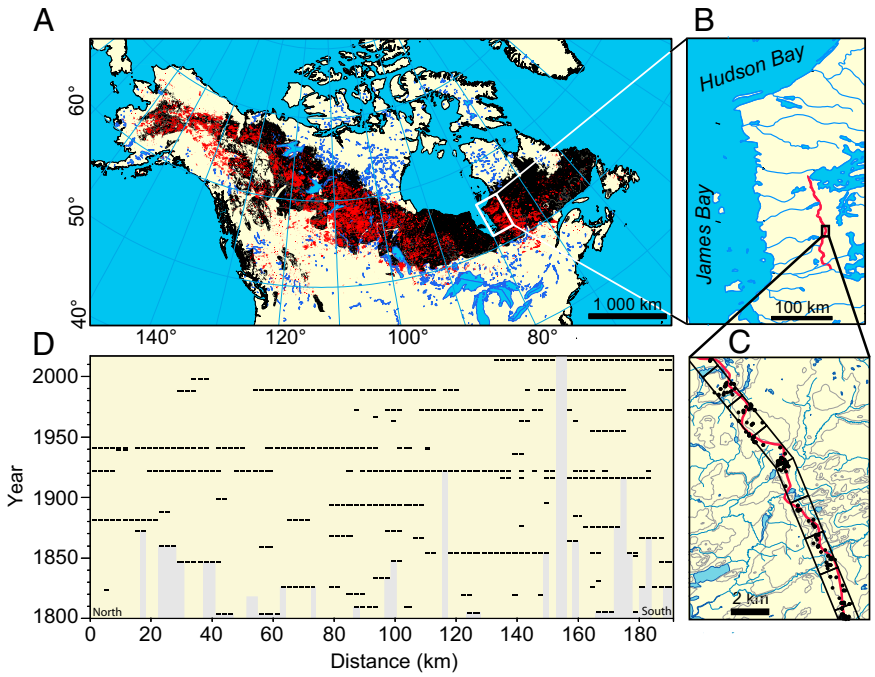

Fig. 1. Fire in space and time across the North American boreal forest. (*A*) Recent (1980–2010) fire polygons (26, 27) (*red*) superimposed onto the unlogged areas (*black*) of the boreal forest according to the Frontier Forests map (34). (*B*) Studied road transect in eastern Canada. (*C*) Section of the transect showing adjoining 2 × 1 km cells, along with sampled trees (*dots*). (*D*) Fire overlaps along the transect during the1800–2013 period retained for analysis (Fig. S3 and Dataset S1 give the complete fire record). Each dash represents a fire detected inside a 2 km^2 cell. The gray shading displays the nonrecording period of each cell.

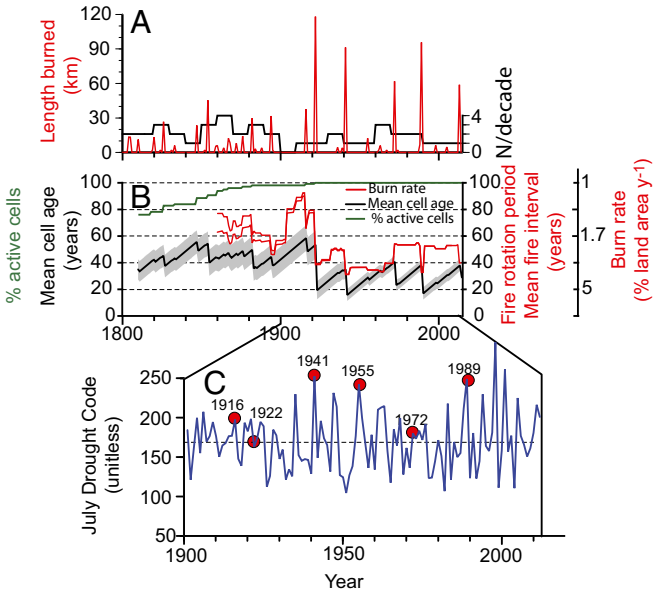

Fig. 2. Effect of drought-induced fires on burn rates and forest age. (*A*) Length burned per year (*red line*) and number of fire years per decade (*black line*). (*B*) Burn rate and its inverse, the fire rotation period. The upper and lower red lines represent the raw burn rate and the burn rate weighed by the percentage of active cells, respectively. The fire rotation period also corresponds to the mean fire interval across all cells. The forest mean age, computed yearly by averaging the TSF across all cells, is displayed with its 95% confidence interval (*shading*). (*C*) July mean DC. Red circles indicate years with fires longer than 10 km; horizontal dashed line indicate the mean DC during the 1901–2012 period.

forests can burn during extreme fire years (Fig. 1*D*). However, when a territory larger than the largest possible fire is considered over multiple fire overlap–fuel recovery episodes, thus encompassing a large fraction of the natural range of variability, these short FIs are less likely than longer ones (Fig. 3*C*). Indeed, short FIs were mainly generated by fire overlaps at the margin of previous large fires (e.g., 1989 vs. 1972 in Fig. 1*D*). For example, the third largest fire (5,830 km^2) recorded in Canada since 1980 occurred in our study area in June–July 2013 (Fig. S2). Although the fire overlapped some areas previously burned in 1983, 1989, and 2005, it mostly burned older forest stands (older than 41 y). Collectively, these results indicate that even if severe droughts continue to occur, overabundant young forest stands will provide resistance against increasing fire size and decreasing FIs.

Fire data for the rest of the North America boreal zone indicate that the negative feedback observed across our study area is operating to limit high burn rates at the continental scale. Fire overlaps observed during the 1980–2010 period were about half as frequent as would be expected by chance, especially for burn rates greater than 1% y^{-1}, emphasizing a fuel-dependent limitation on burn rates and fire overlaps, at least for FI shorter than the record's length of 31 y (Fig. 5). This resistance against more fire is systematic across the unmanaged boreal zone and is highly statistically significant (Fig. 5 and Fig. S4). Assuming that burn rates higher than 1% are constrained to some degree through a stand-age feedback, then about 700,000 km^2 of boreal forest would be fuel-limited, mostly in the northernmost, unmanaged part of the biome (39). Although the commercial boreal forest is more productive, and potentially less fuel-limited, than its unmanaged counterpart, it is also less exposed to high burn rates because fires are by far more frequent in the unmanaged sector (Fig. 1*A*).

We studied the stand-age feedback without considering fuel composition and productivity. Recent empirical evidence suggests that changing burn rates and burn severities will shift forest composition and productivity, potentially modifying, either positively or negatively, feedbacks on burn rates. For example, in our study area, jack pine (*Pinus banksiana* Lamb.) greatly increased in abundance after the relatively short FI between the large 1941 and 1989 fires (12, 40). Because jack pine has faster juvenile growth than black spruce [*Picea mariana* (Mill.) BSP.], the other common species in this region, a sustained pine increase over time could lead to even more fires in young stands, thereby weakening the negative feedback. Conversely, in some parts of the boreal forest, the abundance of aspen (*Populus tremuloides* Michx.), a broadleaved taxon less flammable than conifers, has been shown to increase after severe fires (14). As large fires are generally more severe than small ones (19), models predict than aspen abundance will increase in a future with more fires, thus potentially strengthening the negative feedback on burn rates (15, 41, 42). Boreal forest productivity may also increase or decrease directly with climate change (43–45), further suggesting the negative feedback on burn rates may not be stationary through time. Geographic differences may also exist across the boreal biome.

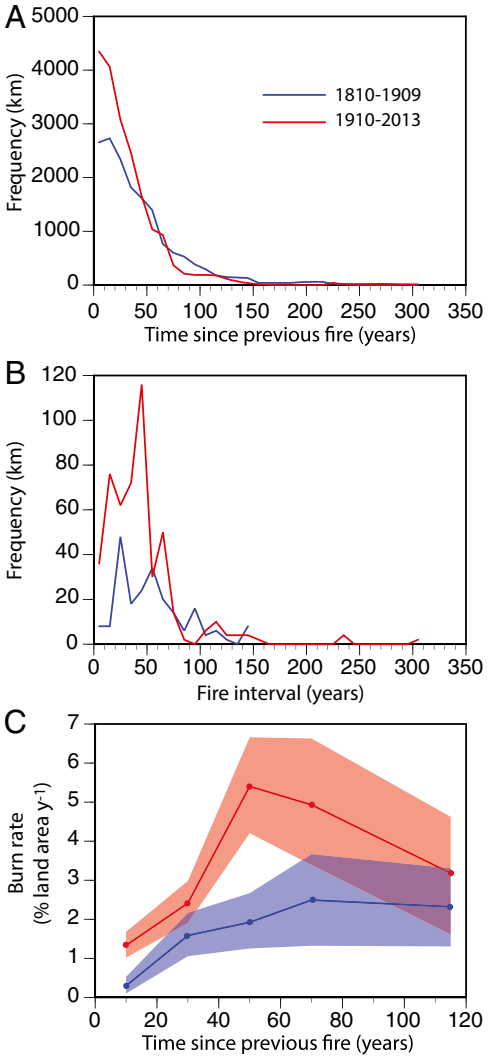

Fig. 3. Burn rate as a function of TSF during the 19th and 20th centuries. (*A*) Frequency distribution of all TSF that have occurred along the transect over the 1810–1909 and 1910–2013 periods. (*B*) Frequency distribution of all fire intervals that ended during each period. (*C*) Burn rate according to the TSF, as determined from the ratio of *B* over *A*. Bootstrapped 95% confidence intervals are also shown (*shaded*).

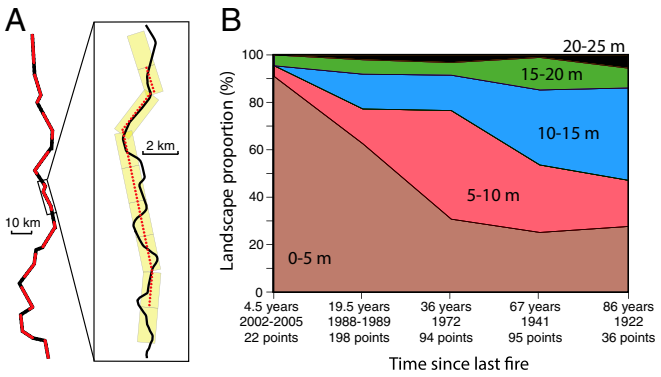

Fig. 4. Landscape variability of forest canopy height according to TSF. (*A*) Location of the sampled points (*red dots*) every 200 m along the road transect. (*B*) Frequency across the study area of the successive 5-m forest canopy height classes as a function of the TSF. Corresponding fire years and numbers of points considered are indicated along the category axis. Frequency and dominance of tree species at the sampled points are given in Table S1.

For example, the larch-dominated Eurasian boreal forest is characterized by different forest composition and fire behavior than the North American boreal forest (46) and probably exhibits different types of fuel feedback.

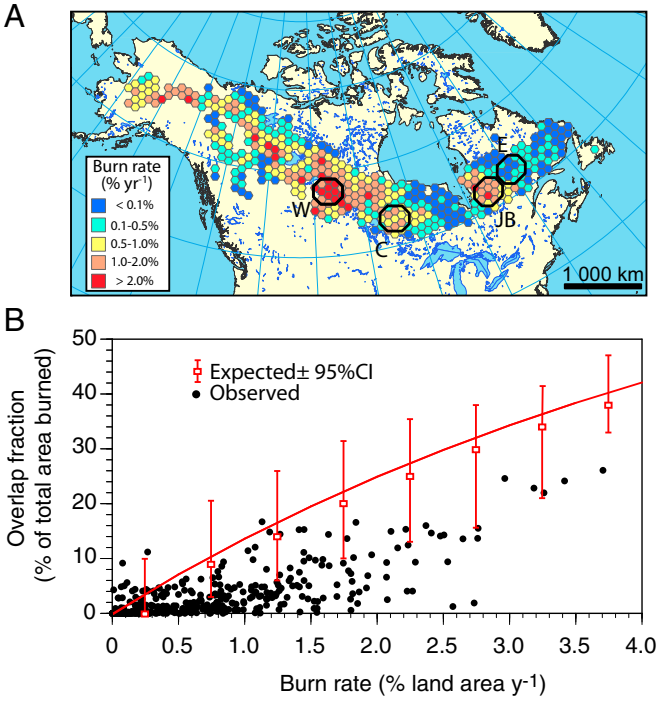

Fig. 5. Burn rates and fire overlaps across the North American boreal forest. (*A*) Burn rates (percentage of the land area burned per year) computed for 8,660 km^2 hexagonal cells, according to fires recorded in Alaska and Canada between 1980 and 2010 (26, 27). Only cells with more than 4,000 km^2 of unlogged forest are considered (34). (*B*) Overlap fraction (percentage of total area burned where two fires overlap) as a function of burn rate for the 406 hexagons considered. The overlap fraction expected under the assumption of random fire occurrence, and its 95% confidence interval, have been estimated after 500 random permutations of the fire polygons centroids within the four octagonal cells shown in *A* (see *Methods* and Fig. S4). W, C, JB, and E refer to octagon locations (West, Central, James Bay, East). The expected overlap fraction computed deterministically from a negative exponential model of forest survivorship with constant burn rate over a 31-y period is also shown (*red line*).

This study sheds light on the opposing roles of extreme weather and stand age on fire recurrence in the North American boreal forest. It thus has important implications for predicting the burn rates and climate change effects of the coming decades. The concern regarding the prediction of large-scale shifts in burn rates is justified, given that large fires prompted by only a few years of extreme drought may be sufficient to abruptly shift fire regimes to extreme burn rates and to maintain these rates over at least a century, as exemplified by the recurrence of very large fires in our study area during the 20th century. However, because of overabundant young forest stands, burn rates are already fuel-limited over large expanses of the unmanaged North American boreal forest, such that the most fire-prone regions would resist further fire-mediated climate change. Therefore, projections of high burn rates (i.e., rates > 1% y^{-1}) during the coming decades are likely to be overestimated, if not constrained by postfire fuel availability. These fire-prone, fuel-limited regions provide reference conditions for evaluating the most extreme fire effects of the coming decades.

Methods

Dating Fires Within Cells Along the Road Transect. The studied north–south transect spans 190.2 km along the James Bay road in northern Québec, Canada (Fig. 1B and Fig. S2). A homogeneous suite of low hills and depressions characterizes this region, which is about 250–350 m above sea level. The region experiences large stand-replacing fires and is strongly dominated by even-aged stands of black spruce and jack pine (Table S1), two species that recover rapidly from crown fire because of their serotinus cones. Eastern larch [*Larix laricina* (Du Roi) K. Koch] is also relatively frequent but rarely dominant. Broadleaved taxa (aspen and paper birch [*Betula papyrifera* Marsh.)] occur in less than 5% of the landscape. The road was built in 1972. The region is not logged, and fires are not suppressed.

Although fires of the North American boreal forest are generally stand-replacing, virtually all fires leave scars on numerous surviving trees at the margin of unburned forest patches or within areas that experience localized surface fire (Fig. S1). Our field method is based on the reasoning that if a sufficiently large sampling cell is carefully surveyed, it would be possible to reconstruct the sequence of fires that have spread across this cell during the last few centuries, using fire scars and establishment dates of trees. A preliminary survey indicated that cells of 2 km^2 would comprise several live and dead scarred stems, often with multiple scars, which would allow dating fire events during the last 200–300 y. Accordingly, the entire transect has been subdivided into 93 adjacent, 2 × 1 km cells (Fig. 1 *B* and *C*). Seven cells have been shortened (mean length ± SD = 1.59 ± 0.25 km), and 12 cells have been elongated (2.59 ± 0.46 km) to adjust the transect shape to the sinuous road path. The center line of each cell had to be no greater than 1 km from the road to facilitate sampling.

Each cell was exhaustively surveyed to locate fire scars on live trees, snags, or woody debris, which tend to be grouped near permanent features that limit fire spread (streams, lakes, peat lands, rocky outcrops, topographic breaks). Two adjacent cells around kilometer 155 were not sampled because of extensive anthropogenic forest clearing (Fig. 1*D*). Two to six scarred stems were sampled at each scar grouping, with the goal of duplicating as many distinct fire years as possible within each cell. Large stems with multiple scars were always preferred over isolated scars, as they are more likely to record short fire intervals. Isolated scars were sampled when additional fires were suspected. A few scars were also sampled at no more than 500 m outside cells. Fire scars from live trees were dated after documented dendrochronological procedures (47). Scars on dead individuals were dated after cross-dating tree ring width patterns using species-specific master ring width chronologies from the study area (48).

Jack pine seedlings establish massively and grow rapidly after fire (12, 22, 40). As a consequence, the first tree ring in a stem cross-section close to the root collar may confirm fires already identified from scars or help identify additional fires, especially after a short fire interval, when small trees are unlikely to survive and develop a scar. We have considered cross-sections with pith taken less than 1 m above the root collar in live pines or dead individuals with an attached stump that were sampled for fire scars. Supplementary unscarred specimens were sampled for their first tree ring only when a new fire date was suspected. The year of the first tree ring at root collar was estimated from the first tree ring at sampling height, with a correction for the time lag between these two levels: C = 0,154 H, where C is the correction (years) as a function of the sampling height H (cm). This regression ($P < 0,0001$; df = 39) has been calibrated from the subset of samples

with attached stumps at sites with precisely known fire dates. To prevent a corrected year from preceding the corresponding fire year, sampled heights were first divided into 2-cm intervals and the regression then calibrated on the fifth percentile of all time lags observed for each interval. In total, our study is based on 1,146 fire dates from scars and 690 dates from corrected first tree rings (Dataset S1 and Fig. S3). To complete and validate our data set, we compared fire records among all pairs of adjacent cells and exhaustively resampled cells with suspected incomplete records or with records not extending into the 18th century.

To be valid, a fire year in a given cell had to be replicated by at least one scar or one first tree ring from the same cell or from one of the two adjacent cells. A cell was considered as active for recording fires for the period after its first valid fire year. Although the proportion of active cells decreases rapidly with increasing time before the 19th century (Table S2), two analyses suggest our database is fairly complete after 1810; that is, for the period with >75% active cells (76% were active in 1810, 89% in 1850, and 100% in 1922; Fig. 2*B*), and that more recent burning has not completely destroyed earlier fire evidence during the last 200 y. First, we verified whether the reconstructed fire lengths include a larger proportion of gaps in fire extent as we go back in time. An index of fire discontinuity (IFD) for fire years with discontinuous series of burned cells was computed from the ratio of the number of unburned cells to the number of burned cells. Burned segments more than 10 km apart for a given fire year were considered independent fire events. Except for an 1854 burn that was highly discontinuous around kilometers 160–180 (Fig. 1*D*; IFD = 1 unburned cell per burned cell), the IFD is stable over the 1811–2008 period and significantly lower than for the 18th century (IFD of 0.1–0.3 vs. 0.3–0.8; Mann–Whitney *U* test; $P < 0.01$; Fig. S5), suggesting the fire record is reasonably complete for the last two centuries. Second, the number of fires recorded per cell is not correlated between the 1810–1909 and 1910–2013 periods (Gamma correlation coefficient = 0.18; $P > 0.05$; $n = 91$), suggesting that an increasing number of recorded fires during the 20th century do not systematically reduce the probability of detecting a fire during the 19th century. Because the most recently inactive cells are scattered along the road transect, large fires could be clearly reconstructed, even during the 18th century, as exemplified by the 1733 fire at cells 1–18 and the 1760 fire at cells 65–92 at the southern and northern ends of the transect, respectively (Fig. S3).

Computing Burn Rates from Fire Lengths. Because we have reconstructed the length of past fires, including fires that were later overlapped by a subsequent burn, burn rates were computed directly from the fire lengths along the transect. For each 50-y time period lagged by 1 y (1810–1859, 1811–1860, ..., 1964–2013), the burn rate (percentage of land area per year) was computed as the product of 100% and the total length burned, divided by the product of the transect length (190.2 km) and the time interval duration (50 y). These burn rates were considered comparable to rates that would have been computed from the surface area of fire polygons (Fig. S6).

Stand Age and the Probability of Burning. We directly reconstructed the TSF each year of each cell from the overlapping sequence of fires over the entire transect. Similarly, FIs between pairs of consecutive fires into each cell could be directly reconstructed from fire overlaps. We then compiled the cell frequency for the same TSF and FI classes (1–20, 21–40, 41–60, 61–80, and 81–150 y) for two consecutive periods (1810–1909 and 1910–2013). To determine how the burn rate varied with TSF during each of these periods, we computed the ratio of the FI over the TSF frequencies by age class, as these frequencies represent the number of cells that burned relative to the number available to burn into each class, respectively. Confidence intervals were estimated by bootstrapping. For each age class, the FI/TSF ratio was computed 10,000 times from random samples of the original data (with replacement), and the 95% confidence limits were estimated from the 2.5% and 97.5% percentiles.

Stand Age and Fuel Loading. We described the postfire trend of fuel recovery from measurements of forest canopy height at points systematically located every 200 m along 135 km of our 190-km transect (Fig. 4*A*). From the 675 points potentially available, 166 occurred in lakes or in disturbed areas (road, cleared areas) and were excluded. Canopy height was visually categorized in 5-m classes (0–5 m, 5–10 m, etc.) at the remaining 509 points. We also determined TSF at each point from recent fire polygons (period 1980–2010) and from our reconstruction of fire overlaps (earlier fires). Considering that some TSF were poorly replicated among points, we finally retained 445 points belonging to five TSF classes (4.5, 19.5, 36, 67, and 86 y) and corresponding to the 2002–2005, 1988–1989, 1972, 1941, and 1922 fire years, respectively (sampling year is 2008).

Drought Index. We verified whether or not the largest fires (fires longer than 10 km) were associated with drought conditions. The DC of the Canadian Forest Fire Weather Index System is a daily index of the moisture content of the deep layers of the forest floor. A recently developed monthly version of the DC is a good predictor of the area burned annually during the last 30–40 y across the Canadian boreal forest (35). We computed the July monthly DC for the 1901–2012 period, using Climate Research Unit total monthly precipitation and monthly averages of daily maximum temperature data (Climate Research Unit time series 3.21 data) (49) and the program SimMDC, written in the R language (35). As the Climate Research Unit data were interpolated into 0.5° latitude by 0.5° longitude grid cells, we computed the mean July DC for an area comprising 16 cells between longitude 52° and 54° W and latitude 76.5° and 78.5° N.

Fire Overlaps at the Continental Scale. We evaluated the null hypothesis that recent fires have overlapped at random (i.e., without age dependence) across the North American boreal forest. Fire polygons for the period 1980–2010 were acquired from the Canadian National Fire Database (26) and the Bureau of Land Management of the Alaska Fire Service (27). Burn rates and fire overlaps (total area reburned) were computed for contiguous hexagonal cells (area of 8,660 km^2 corresponding to a minimum diameter of 100 km), excluding fire < 200 ha, as well as burned areas intersecting water bodies >1 km^2 (Fig. 5*A*). To minimize interactions with logging, we also excluded all cells with less than 4,000 km^2 intact boreal forest according to the Frontier Forests map (34). The observed overlap fraction (the fraction of the total area burned corresponding to fire overlaps) was plotted against the burn rate for each of the 406 remaining hexagons and compared with the fraction expected under the assumption of random fire occurrence (Fig. 5*B*).

The expected overlap fraction and its 95% confidence interval were estimated using random permutations of fire polygons centroids. Four large octagonal cells (106,100 km^2) were located in regions of homogeneous fire size and density without large water bodies, along a gradient of burn rates representative of the North American boreal zone (Fig. 5*A*). These octagons included from 83 to 454 fire polygons and had overall burn rates varying from 0.1% y^{-1} to 2.4% y^{-1} during the 1980–2010 period (Fig. S4*A*). After each of 500 random permutations of the fire polygon centroids within each octagon, the burn rate and overlap fraction were recomputed inside the central hexagonal cell of each octagon. We then combined the 2,000 permutations from all octagons and divided the resulting data set into 8 equal burn rate intervals (Fig. S4*B*). For each central value of these consecutive burn rate intervals, we estimated the expected overlap fraction and its 95% confidence interval from the median of the corresponding permutations and the associated 2.5th and 97.5th percentiles, respectively.

ACKNOWLEDGMENTS. We thank P.-Y. l'Héreault, É. Tremblay, B. Dy, C. Gilbert, R. Terrail, Y. Neveu, A.-M. Labrecque, and V. Hébert-Gentile for help with fieldwork. Funding was provided by Natural Sciences and Engineering Research Council of Canada, the FRQNT (Fonds de recherche du Québec-Nature et technologies), and the Northern Scientific Training Program (Aboriginal Affairs and Northern Development Canada). The town of Radisson offered lodging facilities. We are grateful to M.-P. Girardin, S. Payette, and M. Simard for critically reading earlier versions of the manuscript.

1. Paine RT, Tegner MJ, Johnson EA (1998) Compounded perturbations yield ecological surprises. *Ecosystems (N Y)* 1(6):535–545.
2. Turner MG (2010) Disturbance and landscape dynamics in a changing world. *Ecology* 91(10):2833–2849.
3. Johnson EA (1992) *Fire and Vegetation Dynamics: Studies from the North American Boreal Forest* (Cambridge Univ Press, Cambridge, UK).
4. Payette S (1992) Fire as a controlling process in the North American boreal forest. *A Systems Analysis of the Global Boreal Forest*, eds Shugart HH, Leemans R, Bonan GB (Cambridge Univ Press, Cambridge, UK), pp 144–169.
5. Bond-Lamberty B, Peckham SD, Ahl DE, Gower ST (2007) Fire as the dominant driver of central Canadian boreal forest carbon balance. *Nature* 450(7166):89–92.
6. Balshi MS, et al. (2009) Assessing the response of area burned to changing climate in western boreal North America using a Multivariate Adaptive Regression Splines (MARS) approach. *Glob Change Biol* 15(3):578–600.
7. Bergeron Y, Cyr D, Girardin MP, Carcaillet C (2010) Will climate change drive 21st century burn rates in Canadian boreal forest outside of its natural variability: Collating global climate model experiments with sedimentary charcoal data. *Int J Wildland Fire* 19(8):1127–1139.

8. Flannigan MD, Logan KA, Amiro BD, Skinner WR, Stocks BJ (2005) Future Area Burned in Canada. *Clim Change* 72(1-2):1–16.
9. Boulanger Y, Gauthier S, Burton PJ (2014) A refinement of models projecting future Canadian fire regimes using homogeneous fire regime zones. *Can J Res* 44(4):365–376.
10. Kasischke ES, Turetsky MR (2006) Recent changes in the fire regime across the North American boreal region–spatial and temporal patterns of burning across Canada and Alaska. *Geophys Res Lett* 33(9):L09703.
11. Ali AA, et al. (2012) Control of the multimillennial wildfire size in boreal North America by spring climatic conditions. *Proc Natl Acad Sci USA* 109(51):20966–20970.
12. Lavoie L, Sirois L (1998) Vegetation changes caused by recent fires in the northern boreal forest of eastern Canada. *J Veg Sci* 9(4):483–492.
13. Girard F, Payette S, Gagnon R (2008) Rapid expansion of lichen woodlands within the closed-crown boreal forest zone over the last 50 years caused by stand disturbances in eastern Canada. *J Biogeogr* 35(3):529–537.
14. Johnstone JF, Hollingsworth TN, Chapin FS, Mack MC (2010) Changes in fire regime break the legacy lock on successional trajectories in Alaskan boreal forest. *Glob Change Biol* 16(4):1281–1295.
15. Johnstone JF, Rupp TS, Olson M, Verbyla D (2011) Modeling impacts of fire severity on successional trajectories and future fire behavior in Alaskan boreal forests. *Landscape Ecol* 26(4):487–500.
16. Boiffin J, Munson AD (2013) Three large fire years threaten resilience of closed crown black spruce forests in eastern Canada. *Ecosphere* 4(5):56.
17. Balshi MS, et al. (2009) Vulnerability of carbon storage in North American boreal forests to wildfires during the 21st century. *Glob Change Biol* 15(6):1491–1510.
18. Kurz WA, Stinson G, Rampley GJ, Dymond CC, Neilson ET (2008) Risk of natural disturbances makes future contribution of Canada's forests to the global carbon cycle highly uncertain. *Proc Natl Acad Sci USA* 105(5):1551–1555.
19. Turetsky MR, et al. (2011) Recent acceleration of biomass burning and carbon losses in Alaskan forests and peatlands. *Nat Geosci* 4:27–31.
20. Kashian DM, Romme WH, Tinker DB, Turner MG, Ryan MG (2013) Postfire changes in forest carbon storage over a 300-year chronosequence of Pinus contorta-dominated forests. *Ecol Monogr* 83(1):49–66.
21. Brown C, Johnstone J (2011) How does increased fire frequency affect carbon loss from fire? A case study in the northern boreal forest. *Int J Wildland Fire* 20(7): 829–837.
22. Arseneault D (2001) Impact of fire behavior on postfire forest development in a homogeneous boreal landscape. *Can J Res* 31(8):1367–1374.
23. Brown CD, Johnstone JF (2012) Once burned, twice shy: Repeat fires reduce seed availability and alter substrate constraints on Picea mariana regeneration. *For Ecol Manage* 266:34–41.
24. Johnstone JF, Chapin FS (2006) Fire interval effects on successional trajectory in boreal forests of northwest Canada. *Ecosystems (N Y)* 9(2):268–277.
25. Buma B, Brown CD, Donato DC, Fontaine JB, Johnstone JF (2013) The impacts of changing disturbance regimes on serotinous plant populations and communities. *Bioscience* 63(11):866–876.
26. Canadian Forest Service (2014) Canadian Wildland Fire Information System. Available at http://cwfis.cfs.nrcan.gc.ca/datamart. Accessed August 19, 2014.
27. Alaska Interagency Coordination Center (2014) Fire History In Alaska. Available at http://afsmaps.blm.gov/imf_firehistory/imf.jsp?site=firehistory. Accessed August 19, 2014.
28. Bessie WC, Johnson EA (1995) The relative importance of fuels and weather on fire behavior in subalpine forests. *Ecology* 76(3):747–762.
29. Parisien MA, et al. (2014) An analysis of controls on fire activity in boreal Canada: Comparing models built with different temporal resolutions. *Ecol Appl*, 10.1890/13-1477.1.
30. Schimmel J, Granström A (1997) Fuel succession and fire behavior in the Swedish boreal forest. *Can J Res* 27(8):1207–1216.
31. Niklasson M, Granström A (2000) Numbers and sizes of fires: Long–term spatially explicit fire history in a Swedish boreal landscape. *Ecology* 81(6):1484–1499.
32. Higuera PE, Brubaker LB, Anderson PM, Hu FS, Brown TA (2009) Vegetation mediated the impacts of postglacial climate change on fire regimes in the south-central Brooks Range, Alaska. *Ecol Monogr* 79(2):201–219.
33. Lynch JA, Clark JS, Bigelow NH, Edwards ME, Finney BP (2002) Geographic and temporal variations in fire history in boreal ecosystems of Alaska. *J Geophys Res* 108(D1):8-1–8-17.
34. Bryant DG, Nielsen D, Tangley L (1997) *The Last Frontier Forests: Ecosystems and Economies on the Edge* (World Resources Institute, Forest Frontiers Initiative, Washington, DC).
35. Girardin MP, Wotton BM (2009) Summer moisture and wildfire risks across Canada. *J Appl Met Clim* 48(3):517–533.
36. Luo Y, Weng E (2011) Dynamic disequilibrium of the terrestrial carbon cycle under global change. *Trends Ecol Evol* 26(2):96–104.
37. Johnson EA, Gutsell SL (1994) Fire frequency models, methods and interpretations. *Adv Ecol Res* 25:239–287.
38. Van Wagner CE (1978) Age–class distribution and the forest fire cycle. *Can J Res* 8(2): 220–227.
39. Boulanger Y, Gauthier S, Burton PJ, Vaillancourt MA (2012) An alternative fire regime zonation for Canada. *Int J Wildland Fire* 21(8):1052–1064.
40. Le Goff E, Sirois L (2004) Black spruce and Jack pine dynamics simulated under varying fire cycles in the northern boreal forest of Quebec. *Can J Res* 34(12):2399–2409.
41. Terrier A, Girardin MP, Périé C, Legendre P, Bergeron Y (2013) Potential changes in forest composition could reduce impacts of climate change on boreal wildfires. *Ecol Appl* 23(1):21–35.
42. Kelly R, et al. (2013) Recent burning of boreal forests exceeds fire regime limits of the past 10,000 years. *Proc Natl Acad Sci USA* 110(32):13055–13060.
43. Alcaraz-Segura D, Chuvieco E, Epstein HE, Kasischke ES, Trishchenko A (2010) Debating the greening vs. browning of the North American boreal forest: Differences between satellite datasets. *Glob Change Biol* 16(2):760–770.
44. Goetz SJ, Bunn AG, Fiske GJ, Houghton RA (2005) Satellite-observed photosynthetic trends across boreal North America associated with climate and fire disturbance. *Proc Natl Acad Sci USA* 102(38):13521–13525.
45. Girardin MP, et al. (2014) Unusual forest growth decline in boreal North America covaries with the retreat of Arctic sea ice. *Glob Change Biol* 20(3):851–866.
46. de Groot WJ, et al. (2013) A comparison of Canadian and Russian boreal forest fire regimes. *For Ecol Manage* 294:23–34.
47. Falk DA, et al. (2011) Multi-scale controls of historical forest-fire regimes: New insights from fire-scar networks. *Front Ecol Environ* 9(8):446–454.
48. Arseneault D, Boucher É, Bouchon É (2007) Asynchronous forest–stream coupling in a fire–prone boreal landscape: Insights from woody debris. *J Ecol* 95(4):789–801.
49. Jones P, Harris I (2014) High-resolution gridded datasets (and derived products). Available at www.cru.uea.ac.uk/cru/data/hrg/#superseded. Accessed August 19, 2014.